PRECISION MEASUREMENT OF NEUTRON ASYMMETRY A_1^N IN THE VALENCE QUARK REGION

XIAOCHAO ZHENG

Massachusetts Institute of Technology
E-mail: xiaochao@jlab.org

(FOR THE JEFFERSON LAB HALL A COLLABORATION)

We have measured the neutron virtual photon asymmetry A_1^n over the kinematic range $0.33 \leq x \leq 0.61$ and $2.8 \leq Q^2 \leq 4.9$ (GeV/c)^2. To extract A_1^n, longitudinal and transverse spin asymmetries have been measured for inclusive $^3\vec{H}e(\vec{e}, e')$ scattering, using a 5.7 GeV longitudinally polarized electron beam at Jefferson Lab and a high-density polarized ^3He target in Hall A. Preliminary results of A_1^n are presented and compared to existing data and various models, including the predictions of SU(6), broken SU(6) constituent quark models and perturbative QCD based models.

1. Introduction

1.1. A_1^n at large x_{Bj}

In the scattering of polarized electrons on a polarized target, the virtual photon asymmetry A_1 is defined as

$$A_1 = \frac{\sigma^{\uparrow\downarrow} - \sigma^{\uparrow\uparrow}}{\sigma^{\uparrow\downarrow} + \sigma^{\uparrow\uparrow}} \tag{1}$$

where $\sigma^{\uparrow\downarrow}$ and $\sigma^{\uparrow\uparrow}$ are cross sections with virtual photon spin antiparallel and parallel to target spin, respectively. A_1 can be expressed as a ratio of the polarized structure functions g_1, g_2 and the unpolarized structure function F_1 as

$$A_1 = \frac{g_1(x, Q^2) - \gamma^2 g_2(x, Q^2)}{F_1(x, Q^2)} \tag{2}$$

with a kinematic factor $\gamma^2 = \frac{4M^2x^2}{Q^2}$, M the nucleon mass, $x = x_{Bj}$ the Bjorken variable, and Q^2 the four momentum transfer squared.

The value of A_1 in the large x region is of particular interest because valence quarks are presumed to dominate in this region. Hence there is

minimal contribution from sea quarks and gluons to the physics quantities being measured. For the same reason, the constituent quark model is presumed to work fairly well in the large x region. Moreover, for deep inelastic scattering in the large x region where the nucleon momentum is mainly carried by the struck quark, it is possible to do perturbative QCD calculations.

1.2. *Theories about* A_1^n

To first approximation, the constituent quarks in the nucleon are described by SU(6) wavefunction as:

$$|n\uparrow\rangle = \frac{1}{2}|d\uparrow(ud)_{S=0}\rangle + \frac{1}{\sqrt{18}}|d\uparrow(ud)_{S=1}\rangle - \frac{1}{3}|d\downarrow(ud)_{S=1}\rangle$$
$$-\frac{1}{3}|u\uparrow(dd)_{S=1}\rangle - \frac{\sqrt{2}}{3}|u\downarrow(dd)_{S=1}\rangle \quad (3)$$

where the subscript S denotes the total spin of the diquark state. In this limit where SU(6) is an exact symmetry, both diquark spin states $S = 1$ and $S = 0$ contribute equally to the observables of interest, leading to the predictions:

$$A_1^p = \frac{5}{9}, \quad \text{and } A_1^n = 0. \quad (4)$$

However, the SU(6) symmetry is known to be broken. A natural SU(6) symmetry breaking mechanism based on phenomenological arguments is the hyperfine interaction among the quarks, described as $\vec{S}_i \cdot \vec{S}_j\ \delta^3(\vec{r}_{ij})$, where $\vec{S}_i$ is the spin of ith quark. It is this interaction that explains, for example, the difference between the nucleon and Δ masses. The effect of this perturbation on the wavefunction is to lower the energy of the $S = 0$ 'diquarks', allowing the d-quark in the first term of Eq.(3), which has its spin parallel to that of the neutron, to be more energetic and hence to dominate the high energy tail of the quark momentum distribution that is probed as $x \to 1$. The dominance of this term as $x \to 1$ implies:

$$A_1^p \to 1, \quad \text{and} \quad A_1^n \to 1. \quad (5)$$

In the large x region, $A_1^p(x)$ and $A_1^n(x)$ can be calculated based on this mechanism[1].

Another approach focuses directly on relativistic quarks instead of the nonrelativistic quarks in the previous discussion. Farrar and Jackson[2] in the early 1970's, as one of the first applications of pQCD, noted that at $x \to 1$, the scattering is from a high energy quark, and the process can be

treated perturbatively. Farrar and Jackson proceeded to show that a quark carrying nearly all the momentum of the nucleon (i.e. $x \to 1$) must have the same helicity as the nucleon and that quark-gluon interactions cause only the $S = 1$, $S_z = 1$ diquark spin projection component, rather than the full S=1 diquark system to be suppressed as $x \to 1$. This gives $d^{\downarrow} = u^{\downarrow} = 0$, $\frac{d^{\uparrow}}{u^{\uparrow}} \to \frac{1}{5}$ as $x \to 1$. Consequently, they obtained the previous limiting value for both the proton and the neutron, namely $A_1^{n,p} \to 1$ for $x \to 1$. This is one of few places where QCD can make an absolute prediction for the x dependence of the structure functions (here a ratio of structure functions). How low in x and Q^2 this picture will work is uncertain. Using this pQCD prediction as a constraint at $x = 1$, A_1^n can be calculated from polarized and unpolarized parton distributions, for example, LSS parametrization[3]. A similar result is obtained in the treatment of Brodsky, Burkhardt and Schmidt (BBS) based on quark-counting-rules[4].

In addition to SU(6), constituent quark models and pQCD based models, there are a few other models which can give a prediction for A_1^n at large x.

A global next-to-leading order (NLO) QCD analysis of unpolarized and polarized DIS data has been performed based on a statistical model of the nucleon[5], and a good description has been obtained in a broad range of x and Q^2 of all measured structure functions. In this calculation, A_1^p and A_1^n approach certain positive values (smaller than 1) at $x \to 1$.

Using the local quark-hadron duality, the large x behavior of structure functions can be predicted from empirical electromagnetic form factors[6]. In this case, A_1^p and A_1^n approach 1 at $x \to 1$ naturally.

In contrast to other theories, the chiral soliton model[7] and the instanton model[8] predict the possibility that A_1^n can be negative at large x.

However, compared to the various theoretical predictions listed above, all world data for A_1^n at $x > 0.4$ have poor statistics and are consistent with the SU(6) prediction $A_1^n = 0$ and can not even determine the sign of A_1^n. Therefore, high precision data on A_1^n at large x are greatly needed.

2. The Experiment E99-117

2.1. *The Experiment*

The experiment E99-117[9] was carried out in Hall A at JLab in the summer of 2001 to measure A_1^n in the x region $0.33 < x < 0.61$. The kinematics are shown in Table 1. To measure A_1^n, the asymmetries $A_{\parallel}$ and $A_{\perp}$ of polarized e^- scattering off polarized ^3He target have been measured in deep inelastic

Table 1. E99-117 kinematics

x_{Bj}	0.331	0.474	0.609
Q^2 (GeV/c)^2	2.738	3.567	4.887
W^2 (GeV/c)^2	6.426	4.846	4.023

region, which are defined as

$$A_{\parallel} = \frac{\sigma^{\uparrow\Downarrow} - \sigma^{\uparrow\Uparrow}}{\sigma^{\uparrow\Downarrow} + \sigma^{\uparrow\Uparrow}}, \quad A_{\perp} = \frac{\sigma^{\uparrow\Leftarrow} - \sigma^{\uparrow\Rightarrow}}{\sigma^{\uparrow\Leftarrow} + \sigma^{\uparrow\Rightarrow}} \tag{6}$$

where $\sigma^{\uparrow\Downarrow}$, $\sigma^{\uparrow\Uparrow}$, $\sigma^{\uparrow\Leftarrow}$ and $\sigma^{\uparrow\Rightarrow}$ are cross sections with electron spin antiparallel, parallel, anti-perpendicular and perpendicular to target spin, respectively. A_1 can be extracted from $A_{\parallel}$ and $A_{\perp}$ as

$$A_1 = \frac{A_{\parallel}}{D(1+\eta\xi)} - \frac{\eta A_{\perp}}{d(1+\eta\xi)} \tag{7}$$

where D, d, η, ξ are kinematic variables. To reduce the possible systematic errors related to the beam helicity and target polarization directions, data were taken for four different beam helicity and target polarization configurations for parallel settings and two different configurations for perpendicular settings.

2.2. *Experimental Setup*

Fig. 1 shows the floor plan of experimental hall A. The polarized electron beam enters the hall from the left side. Two methods - eP and ARC[10] - were used to measured the beam energy to a level of 3×10^{-4}. Beam polarization was measured by a Møller polarimeter regularly and was continuously monitored by a Compton polarimeter. During the experiment the beam energy was 5.7 GeV and beam polarization was 82%± 2.4%.

At the center of the hall the electron beam interacts with the polarized ^{3}He target. This target is based on the principle of optical pumping of Rubidium (Rb), after which ^{3}He nuclei are polarized by spin exchange in Rb-^{3}He collisions. The target cell is a 25 cm long glass vessel with $\sim 130\ \mu m$ end windows and a ^{3}He density of about 10 atm at room temperature. The target polarization is measured by two independent polarimetries - NMR polarimetry based on the adiabatic fast passage technique[11], calibrated with a water signal and EPR polarimetry which measures the shift in Rb's electron paramagnetic resonance (EPR) frequency due to the polarization of ^{3}He. These two polarimetries provide independent and complementary

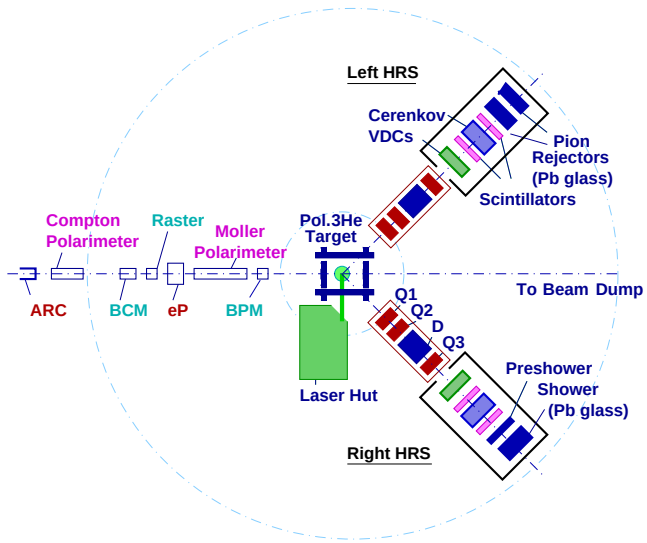

Figure 1. E99-117 floor plan at Jefferson Lab Hall A

measurements of the ^{3}He polarization. During the experiment the average in-beam polarization with an average beam current of 12 μA was 40%± 1.6%.

The scattered electrons were detected by the two standard Hall A High Resolution Spectrometers (HRS)[10] at symmetric positions. Because of the high pion rate and large pion asymmetry in deep inelastic inclusive $\vec{e} - {}^3\vec{H}e$ scattering, the pion rejection efficiency of both HRSs were carefully studied before and during the experiment. Pion rejection was achieved by using a CO_2 gas Cherenkov detector and a double-layered lead-glass shower counter. The combined pion rejection factor was found to be better than 10^4 for both HRSs, with a 99% identification efficiency for electrons. This was sufficient for the kinematical range of this experiment.

3. Data Analysis

3.1. *Extracting Asymmetries*

The raw asymmetries can be extracted from the data as:

$$A_{raw} = \frac{\frac{N^+}{Q^+} - \frac{N^-}{Q^-}}{\frac{N^+}{Q^+} + \frac{N^-}{Q^-}} \tag{8}$$

where N^h and Q^h are the yield and accumulated beam charge for each beam helicity state $h = \pm$. The physics asymmetries $A_\parallel$ and $A_\perp$ are obtained by

$$A_{phys} = \frac{A_{raw}}{f P_b P_t} \tag{9}$$

where f is the target dilution factor, typically 0.92∼0.94, P_b and P_t are the beam and target polarizations. The signs for parallel and perpendicular asymmetries were checked by measuring the ^{3}He elastic asymmetry and the $\Delta(1232)$ asymmetry; both are well known from either theoretical calculation or existing data. False asymmetries were checked by measuring asymmetries of polarized e^- beam scattering off unpolarized ^{12}C foil target. The result shows that the false asymmetry is negligible compared to the physics asymmetry being measured. Finally $A_1^{^3He}$ can be calculated from physics asymmetries using Eq. (7).

3.2. *Radiative Corrections*

Radiative corrections have been applied to the ^{3}He asymmetries $A_\parallel^{^3He}$ and $A_\perp^{^3He}$ directly. Since the theoretical aspects of radiative corrections are mostly understood[12], the uncertainty in the correction is mainly due to the uncertainty in the structure functions used in the procedure. This is studied by using various world fits for the structure functions F_2, g_1, g_2 and the ratio $R = \sigma_L/\sigma_T$ in the procedure of radiative corrections.

3.3. *From ^{3}He to neutron*

A ^{3}He model which includes S, S', D states and pre-existing $\Delta(1232)$ components in the ^{3}He ground-state wave-function[13] has been used for extracting A_1^n from $A_1^{^3He}$. It gives

$$A_1^n = \frac{F_2^{^3He}}{P_n F_2^n (1 + \frac{0.056}{P_n})}[A_1^{^3He} - 2\frac{F_2^p}{F_2^{^3He}} P_p A_1^p (1 - \frac{0.014}{2P_p})], \tag{10}$$

where P_n and P_p are the effective nucleon polarizations of the neutron and the proton inside ^{3}He. A set of values $P_p = -0.028 \pm 0.004$, $P_n = 0.86 \pm 0.02$[14] were used in the correction. Moreover, an extreme case of $P_p = -0.018$, $P_n = 0.897$[15] were used to study the maximum uncertainty due to nucleon polarizations. The E155 fit[16] of $\frac{g_1}{F_1}$ has been used to obtain the proton contribution from A_1^p at $Q^2 = 4(\mathrm{GeV/c})^2$.

4. Preliminary Results

4.1. A_1^n

Preliminary results of A_1^n are shown in Fig. 2, together with the theoretical predictions described in Section 1.2. Existing world data from HERMES

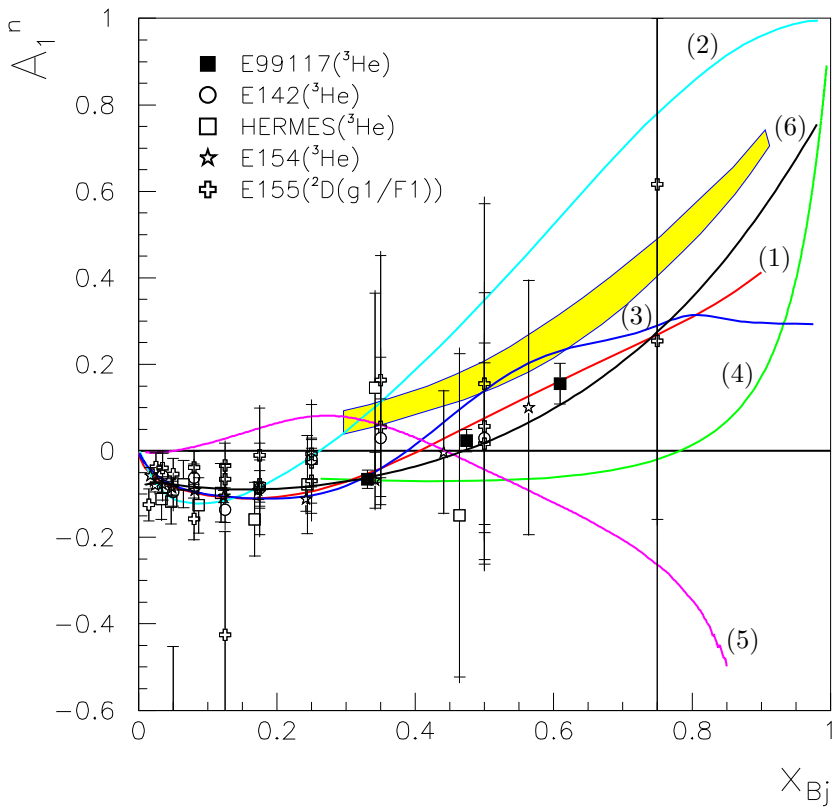

Figure 2. Preliminary result of A_1^n compared with world data and theoretical predictions. Curves: predictions of $\frac{g_1}{F_1}$ from pQCD based model using LSS 2001 parametrization at $Q^2 = 5$ (GeV/c)^2 (1), and A_1^n from constituent quark model (light shaded band), pQCD based model using BBS parametrization (2), statistical model at $Q^2 = 4$ (GeV/c)^2 (3), local duality (4), chiral soliton model at $Q^2 = 3$ (GeV/c)^2 (5), and E155 fit at $Q^2 = 4$ (GeV/c)^2 (6).

and SLAC are also shown. The error bars in Fig. 2 only include statistical errors. However, a detailed study has been done for systematic errors

showing that the total error is dominated by statistics.

Compared with world data, the E99-117 datum at $x = 0.33$ is in good agreement with existing data. In the region of $x > 0.4$, the statistical error of A_1^n has been improved by about a factor of 10. Also, the data show a clear trend that A_1^n turns to positive values at large x. Compared with theory curves, it is important to note that the constituent quark model gives the correct sign and trend of A_1^n at large x. Two other models which use the world data as input - the LSS parametrization and Soffer's statistical model can be largely refined if the data from this experiment are included in the inputs.

4.2. *Other Results*

A preliminary result of g_1^n is obtained by multiplying $\frac{g_1}{F_1}$ data by the F_1 world fit. Similar to A_1^n, the result for g_1^n has improved the statistical error of the world data by about an order of magnitude.

Besides A_1^n and g_1^n, the asymmetry A_2^n and structure functions g_2^n can also be extracted from our data. The statistical uncertainties of A_2^n and g_2^n are about twice as large as that of the latest data from SLAC E155x[17].

4.3. *Pion Asymmetries*

In addition to electron asymmetries in inclusive $^3\vec{H}e(\vec{e}, e')$ scattering, there is a large amount of asymmetry data on pion photoproduction, from E99-117 and other g_1 experiments. Unfortunately, available theoretical calculations of pion asymmetries are rather limited. It has been shown that the pion asymmetry at large pion transverse momentum $\vec{p}_T$ is sensitive to the polarized parton and polarized gluon distributions[18], but there is no such prediction suitable for the JLab energy range. Theoretical work on the pion asymmetry at low and medium energies ($\vec{p}_T$ ~1 GeV/c) is an area where progress should be made to interpret the data.

5. Summary and Outlook

Experiment E99-117 provided precise data on the neutron spin asymmetry A_1^n. Data on the structure functions $g_1^n(x, Q^2)$, A_2^n and $g_2^n(x, Q^2)$ are also available. The results of this experiment will provide valuable input to pQCD based calculations, as well as other models in which neutron data are used as input. A_1^n in the valence quark region is of great interest in the understanding of the valence quark structure, the constituent quark models and the transition between perturbative and non-perturbative regions

of QCD. The measurement of A_1^n in the valence quark region is also an important part of the JLab 12 GeV upgrade[19], in which A_1^n will be measured up to $x = 0.8$ and within a larger Q^2 range of $2 < Q^2 < 10$ (GeV/c)^2.

Acknowledgments

We would like to thank the personnel of Jefferson Lab for their efforts which resulted in the successful completion of the E99-117 experiment, with particular thanks to those in the accelerator division and in Hall A. The work presented was supported in part by funds provided to the Laboratory for Nuclear Science at the Massachusetts Institute of Technology by the U. S. Department of Energy(DOE) under contract number DE-FC02-94ER40818. The Southeastern Universities Research Association operates the Thomas Jefferson National Accelerator Facility for the DOE under contract DE-AC05-84ER40150.

References

1. N. Isgur, *Phys. Rev.* **D59**, 034013 (1999); e-Print: hep-ph/9809255
2. G. R. Farrar, D. R. Jackson, *Phys. Rev. Lett.* **35**, 1416(1975).
3. E. Leader, A. V. Sidorov, D. B. Stamenov, *Eur. Phys. J.* **C23**, 479 (2002); e-Print: hep-ph/0111267
4. E. Leader, A. V. Sidorov, D. B. Stamenov, *Int. J. Mod. Phys.* **A13**, 5573 (1998); e-Print: hep-ph/9708335
5. C. Bourrely, J. Soffer, F. Buccella, *Eur. Phys. J.* **C23**, 487 (2002); e-Print: hep-ph/0109160v1.
6. W. Melnitchouk, *Phys. Rev. Lett.* **86**, 35 (2001); e-Print: hep-ph/0106073
7. H. Weigel, L. Gamberg and H. Reinhardt, *Phys. Lett.* **B399**, 287 (1997); *Phys. Rev.* **D55**, 6910 (1997).
8. N. I. Kochelev, talk presented at the Workshop "Deep Inelastic Scattering off Polarized Targets: Theory Meets Experiment", Sept. 1997, DESY-Zeuthen; e-Print: hep-ph/9711226v1.
9. JLab E99-117, J. P. Chen, Z. -E. Meziani, P. Souder *et al.*, http://hallaweb.jlab.org/physics/experiments/he3/A1n/
10. B. D. Anderson *et al.*, http://hallaweb.jlab.org/equipment/NIM.ps
11. A. Abragam, *Principles of Nuclear Magnetism*, (Oxford University Press 1961).
12. I. Akushevich *et al.*, *Comp. Phys. Comm.* **104**, 201 (1997); e-Print: hep-ph/9706516.
13. F. Bissey *et al.*, *Phys. Rev.* **C65**, 064317 (2002); e-Print: hep-ph/0109069.
14. C. Ciofi degli Atti *et al.*, *Phys. Rev.* **C48**, R968 (1993).
15. A. Nogga, Ph.D. thesis, (2001).
16. P. L. Anthony *et al.*, *Phys. Lett.* **B493**, 19 (2000); e-Print: hep-ph/0007248

17. P. L. Anthony *et al.*, submitted to *Phys. Rev. Lett.*; e-Print: hep-ex/0204028
18. A. Afanasev, C. E. Carlson and C. Wahlquist, *Phys. Rev.* **D58**, 054007 (1998); e-Print: hep-ph/9706522.
19. Jefferson Lab, *The Science Driving the 12 GeV Upgrade of CEBAF*, (2001); http://www.jlab.org/div_dept/physics_division/GeV/WhitePaper_V11.ps